THERYA, 2023, Vol. 14(1):161-179 DOI:10.12933/therya-23-2236 ISSN 2007-3364

Revisiting species delimitation within *Reithrodontomys sumichrasti* (Rodentia: Cricetidae) using molecular and ecological evidence

Elizabeth Arellano[1]*, Ana L. Almendra[1], Daily Martínez-Borrego[1], Francisco X. González-Cózatl[1], and Duke S. Rogers[2]

[1] Centro de Investigación en Biodiversidad y Conservación, Universidad Autónoma del Estado de Morelos. Avenida Universidad 1001, CP. 62209, Cuernavaca. Morelos, México. Email: elisabet@uaem.mx (EA), al.almendra@gmx.com (ALA), daily.marbo@gmail.com (DM-B), xavier@uaem.mx (FXG-C).

[2] Life Science Museum and Department of Biology, Brigham Young University. CP. 84602, Provo. Utah, U.S.A. Email: duke_rogers@byu.edu (DSR).

*Corresponding author: https://orcid.org/0000-0001-8709-9514.

Reithrodontomys sumichrasti is distributed from central México to Panama. Previous studies using DNA sequences suggest the existence of distinct clades that may deserve species-level recognition. Here, we use multiple methods of species delimitation to evaluate if this taxon is a complex of cryptic species. DNA sequences from the genes Cyt-b, Fgb-I7, and Acp5 were obtained from GenBank to perform molecular analyses. Species boundaries were tested using the bGMYC, STACEY, and BPP species delimitation methods. Divergence times were estimated as well as the Cyt-b genetic distances. We developed Ecological Niche Models and tested hypotheses of niche conservatism. Finally, we estimated the spatiotemporal history of lineage dispersal. The bGMYC proposed two species while STACEY and BPP proposed 4 species (genetic distances ranged from 5.43 % to 7.52 %). The ancestral position of clade I was recovered, with a Pleistocene diversification time within *R. sumichrasti* at ~2.15 Ma. For clade pairwise niche comparisons, the niche identity hypothesis was rejected. The ancestral distribution of *R. sumichrasti* was centered in Central America and spread to the west crossing the Isthmus of Tehuantepec and extending to the mountain regions of Central México. Our taxonomic considerations included the recognition of four clades as distinct species within *R. sumichrasti*.

Reithrodontomys sumichrasti se distribuye desde el centro de México hasta Panamá. Estudios previos con secuencias de ADN sugieren la existencia de clados distintos y su posible reconocimiento como especies. En este estudio, probamos diferentes métodos de delimitación de especies para evaluar si este taxón constituye un complejo de especies crípticas. Las secuencias de ADN de los genes Cyt-b, Fgb-I7 y Acp5 fueron descargadas de GenBank y utilizadas en análisis moleculares. Los límites de especies fueron probados utilizando los métodos de delimitación bGMYC, STACEY y BPP. Se estimaron tiempos de divergencia y distancias genéticas para el gen Cyt-b. Además, construimos Modelos de Nicho Ecológico y probamos hipótesis de conservadurismo de nicho. Finalmente, reconstruimos la historia espaciotemporal de la dispersión de los linajes. El bGMYC propuso dos especies, mientras que STACEY y BPP propusieron 4 especies (las distancias genéticas oscilaron entre 5.43 % y 7.52 %). Se recuperó la posición ancestral del clado I, ubicando en el Pleistoceno la diversificación dentro de *R. sumichrasti*, hace ~2.15 Ma. En las comparaciones de nicho por pares de clados fue rechazada la hipótesis de identidad de nicho. La distribución ancestral de *R. sumichrasti* se centró en América Central desde donde comenzó a extenderse hacia el oeste cruzando el Istmo de Tehuantepec y extendiéndose hacia las regiones montañosas del centro de México. Nuestras consideraciones taxonómicas incluyeron el reconocimiento de cuatro clados como especies distintas dentro de *R. sumichrasti*.

Keywords: Cryptic species; harvest mice; integrative taxonomy; Mesoamerican highlands; phylogeographic patterns.

Introduction

A special issue of Therya dedicated to Dr. Alfred L. Gardner for his long research career on the diversity of neotropical mammals, especially for his work in México, honors this outstanding scientist by contributing important advances to the knowledge of mammalogy. Our contribution adds to the mission of modern systematic biology: the discovery, description, and classification of the biodiversity on the planet from an evolutionary perspective (Daly *et al.* 2012). This task involves subjects under debate over the past three decades, such as the species concept (what a species is) and species delimitation (how a species is recognized). Both subjects are closely related but conveniently divided for practical applications (see review by de Queiroz 2007), and over time, species delimitation has taken priority over species concepts (Sites and Marshall 2003, 2004). Given the current rate of species loss, it is urgent to accurately delimit species inasmuch they are the fundamental unit in studies of ecology, systematic, and conservation biology, among other research areas. From the evolutionary standpoint, species delimitation includes the understanding of population-level mechanisms that can be complex (Huang 2020). Populations differentiation through multiple stages at different rates, in part dependent on factors such as generation time, selection pressure, and gene flow. Tracing the process with an acceptable level of certainty depends on the use of appropriate markers (preferably multiple and independent) and the criteria of evaluation (de Queiroz 2007). One of the most reliable strategies is to use multiple sources of evidence (morphology, genetics, ecology, geography, among others) and to base conclusions on their consistency (Knowles and Carstens 2007; Rissler and Apodaca 2007; Carstens *et al.* 2013).

There are both regions as well as biological groups, which are amenable to test hypotheses about species delimitation. The Mesoamerican region has been repeatedly used as a study model because of its complex physiography and biogeographical history, which is reflected by high biological diversity, including many endemic species (Myers *et al.* 2000), particularly for highland groups. As for groups of organisms, rodents, reptiles, and insects, among others have served as models to test hypotheses about evolutionary patterns and processes (*e. g.* Doody *et al.* 2009; Gilbert and Manica 2015; Maestri *et al.* 2017). Some species of rodents have been assessed by evaluating their phylogenetic relationships and further used to illuminate the vicariant biogeography of Mesoamerica (*e. g.* Sullivan *et al.* 2000; Leon-Paniagua *et al.* 2007; Almendra *et al.* 2018; León-Tapia *et al.* 2021). Such is the case of *Reithrodontomys sumichrasti* (Family Cricetidae; Bradley 2017), with a particular interest in the high levels of intraspecific divergence reported (Sullivan *et al.* 2000; Urbina *et al.* 2006; Hardy *et al.* 2013).

Reithrodontomys sumichrasti is distributed along the highlands of Mesoamerica, from central México at 1,200 masl to Panama above 3,400 masl, inhabiting temperate pine-oak and cloud forests. Seven subspecies are recognized, which are distributed in three disjunctive spots (Hooper 1952; Hall 1981; Figure 1). The range of *R. s. sumichrasti* includes portions of the Sierra Madre Oriental, the Mexican Transvolcanic Belt, and the Oaxacan Highlands (type locality El Mirador, Veracruz, México). The distribution of *R. s. nerterus* is restricted to the west portion of the Mexican Transvolcanic Belt (type locality Nevado de Colima, Jalisco, México) whereas *R. s. luteolus* is found in the Sierra Madre del Sur (type locality Juquila, Oaxaca, México). *R. s. dorsalis* occurs in the mountains of the Mexican states of Chiapas and Guatemala (type locality Tonicapan, Guatemala) and *R. s. modestus* in the highlands of El Salvador, Honduras, and western Nicaragua (type locality Jinotega, Nicaragua). The southernmost distribution of the species includes the Cordillera Central and Cordillera de Talamanca in Costa Rica for *R. s. australis* (type locality Cartago, Costa Rica) and the extreme east of Costa Rica and high mountains of western Panama for *R. s. vulcanius* (type locality Chiriquí, Panama; Hooper 1952).

Previous phylogenetic studies using DNA sequences of the mitochondrial Cytochrome b (Cyt-b) gene (Sullivan *et al.* 2000), or also incorporating the seventh intron of nuclear gene beta-fibrinogen (Fgb-I7) and the second intron of the acid phosphatase type V (Acp5; Hardy *et al.* 2013) have

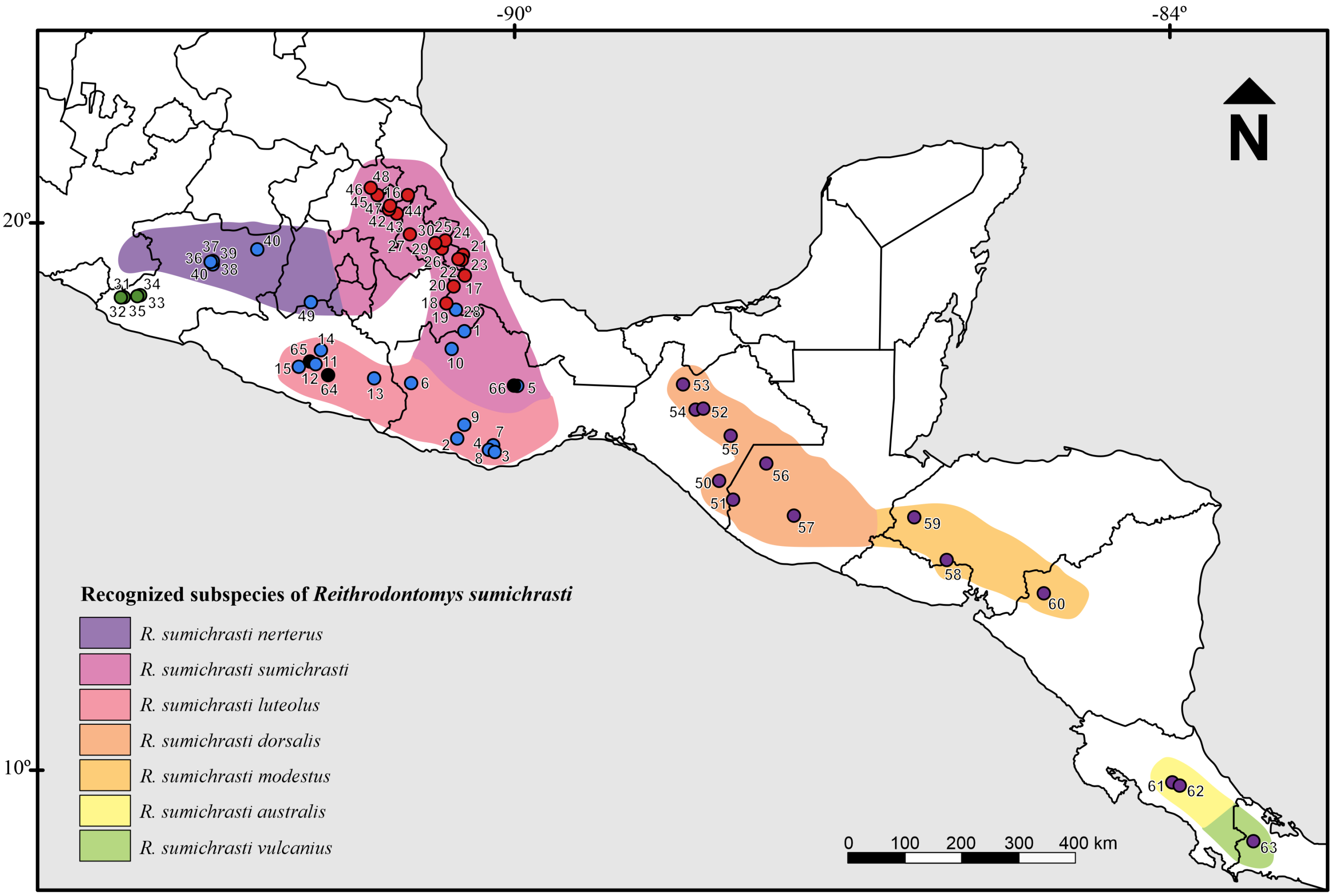

Figure 1. Map of México and Central America (adapted from Hall [1981] and Hardy *et al.* [2013]) showing geographic distribution of the seven recognized subspecies of *Reithrodontomys sumichrasti*. Dots represent the localities used in this study and follow the clade-color distinction described in Figure 2.

revealed the existence of several distinct clades that may deserve species-level recognition. Lineages on either side of the Isthmus of Tehuantepec in México were proposed as distinct biological species, but this pattern has been supported by only mtDNA sequences (Sullivan *et al.* 2000; Hardy *et al.* 2013). Although it was difficult to elucidate the relationships among networks of populations from central México (Hardy *et al.* 2013; Figure 2), there was a clear pattern of phylogenetic structure.

Here, we evaluate species delimitation within *R. sumichrasti* using different methods of analysis than those previously employed to test the hypothesis that *R. sumichrasti* represents a complex of cryptic species. We also comment on the diversification processes in the region and make taxonomic suggestions.

Materials and methods

Data acquisition. DNA sequences from the mitochondrial gene Cyt-b, and the Fgb-I7 and Acp5 nuclear genes, representing Hardy *et al.* (2013) populations dataset of *Reithrodontomys sumichrasti* (*n* = 226) were obtained from GenBank. We sequenced an additional 11 specimens of *R. sumichrasti*, five of these from three new geographic localities (64 to 66; Appendix 1). Given the current availability of sequence data for outgroup taxa, we included samples of *R. zacatecae, R. megalotis*, *R. chrysopsis*, *R. humulis*, *R. montanus*, and *R. raviventris* from the *R. megalotis* species group (Musser and Carleton 2005). The updated DNA datasets were realigned with MAFFT v7 [L-INS-i refinement, gap penalty = 3, offset = 0.5] (Katoh *et al*. 2005) for nuclear markers, and manually for Cyt-b using Geneious Pro v6.1.6 (https://www.geneious.com). The optimal partition scheme (by gene) and models of nucleotide substitution (Cyt-b: GTR+I+G, Fgb-I7: HKY+I+G, Acp5: K80+I+G); were determined with Partition Finder (Lanfear *et al.* 2014).

Phylogenetic hypothesis. We considered the phylogenetic relationships proposed by Hardy *et al.* (2013) as our working hypothesis, where two geographic clades are supported as species-level lineages. One species (spA) split ~2.5 million years ago (Ma) and comprises populations from Chiapas south into Central America (clade I; Figure 2). Species (spB) includes 3 haplogroups restricted to México, west of the Isthmus of Tehuantepec (Figure 2), whose most recent common ancestor was placed ~1.36 Ma (see Hardy *et al.* 2013). To assess support for this phylogenetic hypothesis (Hardy *et al.* 2013), and for alternative topological arrangements, we applied three methods for assessing species boundaries and species tree estimation (see below) that do not require a guide topology or species assignments to be specified a priori.

Single locus species delimitation. A time-calibrated Bayesian Inference (BI) analysis of Cyt-b for *R. sumichrasti* samples was run in BEAST2 v.2.6.2 (Bouckaert *et al.* 2014). We employed a prior rate of evolution of 0.017 substitutions per site per million years (Arbogast *et al.* 2002) and fossil calibrations (*R. moorei*, *R. wetmorei*, *R. galushai*, *R. pratincola*, *R. rexroadensis*, and *R. sp.*) with an offset of exponential prior for the age (in Ma) of the root (mean = 2.25, offset = 1.3, HD = 95 % between 1.5 to 5.5 Ma; Dalquest 1978; Czaplewski 1987; Martin *et al.* 2002; Morgan and White 2005; Lindsay and Czaplewski 2011; Martin and Peláez-Campomanes 2014). BI analysis consisted of four Markov chain Monte Carlo (MCMC) chains of 10 million generations, sampling trees every 1,000 generations and with a burn-in of 20 % of the trees. The last 100 trees sampled from each run were analyzed with 1 million generations of the Bayesian General Mixed Yule-Coalescent (bGMYC) model (Reid and Carstens 2012) in the computing environment R (R Core Team 2018). As advised by Reid and Carstens (2012), outgroup taxa were not included in this analysis. For all Bayesian analyses reported herein, stabilization and appropriate Effective Sample Sizes (ESS ≥ 200) of the posterior distributions for model parameters were examined in Tracer 1.8 (Rambaut *et al.* 2018).

Time-calibrated multiple loci species delimitation. The multiple loci multiple species dataset was analyzed simultaneously with the multi-tree multi-species coalescent method (Heled and Drummond 2010) and the assignment-free species delimitation technique implemented in STACEY (Jones 2017), using BEAST2. The search strategy implemented in STACEY uses a birth-death-collapse prior to approximate alternative delimitation models and node reheight MCMC move that aims to improve the convergence of the species tree estimation, therefore, its performance is subject to the accuracy of divergence times estimation. As recommended, the analysis was run twice, the second time sampling from the prior only; for 100 million generations, trees were sampled every 5,000 generations. A Fossilized Birth-Death model was set on the speciation rate (Heath *et al.* 2014), time-calibrated as specified above. Topologies and clock rates from individual loci were left unlinked, and substitution rates among branches were drawn from a lognormal distribution with a prior mean rate of 0.017 substitutions per site per million years for the Cyt-b (Arbogast *et al.* 2002).

Clock-like multiple loci species delimitation. We assessed the probability of alternative species delimitation models and species trees with the Bayesian Phylogenetics and Phylogeography method (BPPv3.2; Yang and Rannala 2014). This assumes a Jukes-Cantor evolutionary model (strict molecular clock) and applies a species tree search strategy that is grounded on the Nearest Neighbor Interchange (NNI) algorithm, followed by its characteristic rjMCMC move. Although it accounts for the uncertainty on estimated rates of evolution compared to *BEAST-STACEY, this method is applicable to inter- and intra-species datasets that meet the criteria of having clock-like evolutionary rates. For this analysis, uniform rooted species trees were assumed, with gamma priors for the population size (α, β) of $\Theta = (2, 2000)$ and root age (Tau = τ) $\tau 0 = (4, 2, \text{and } 1)$. The rjMCMC was run with algorithm A11 with fine-tune parameter ε _= 2 (joint

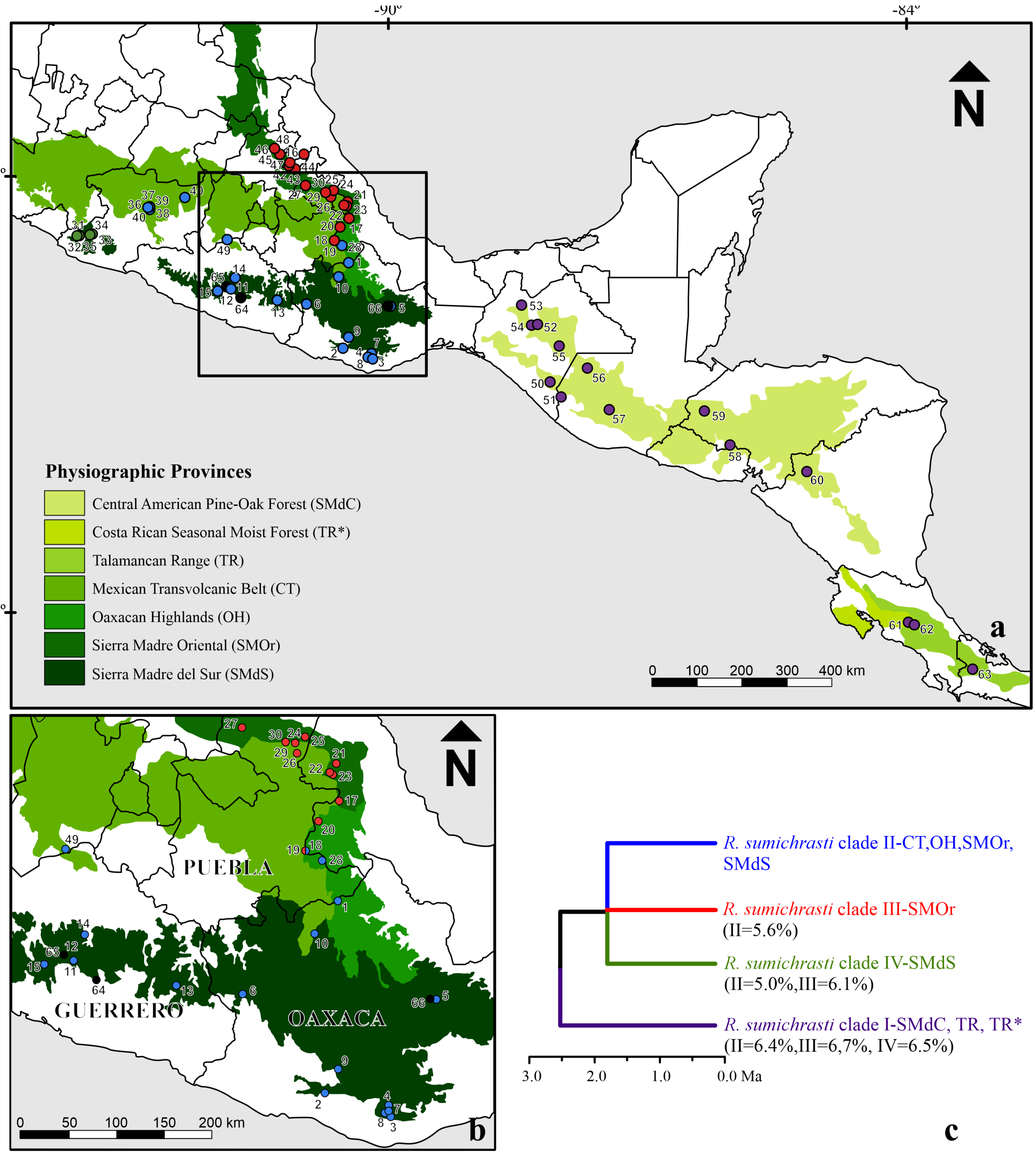

Figure 2. a) Map of México and Central America adapted from Hardy *et al.* (2013) showing collecting localities of *Reithrodontomys sumichrasti* superimposed on a map of the physiographic provinces they occupy. The four clades detected by the authors are demarcated with the colors purple (clade I), blue (clade II), red (clade III), and green (clade IV). Newly incorporated localities are shown as black dots (64-66; Appendix 1). b) Close-up of the area of sympatry of individuals from populations between clade II and clade III. c) Standing time-calibrated phylogenetic hypotheses of the evolutionary relationships among clades within the currently recognized extent of *R. sumichrasti*. Uncorrected Cytochrome-b genetic distances between sister clades are denoted in parentheses as a reference for the level of molecular divergence.

unguided species delimitation and species tree inference) for 500,000 generations with a sampling frequency of 200 after a burn-in period of 10,000.

Genetic distances. Cyt-b genetic distances using the Kimura 2-parameter (K2P; Kimura 1980) and the uncorrected *P*-distances were estimated between and within clades suggested as distinct species using MEGA X (Kumar et al. 2018). This allowed us to make genetic distance comparisons with other values reported for rodents and for *R. sumichrasti* by Bradley and Baker (2001) and Hardy *et al.* (2013), respectively.

Ecological niche equivalence. For each species-level clade (clades I-IV, see Results section), we developed present-time Ecological Niche Models (ENMs) with MAXENT 4. (Phillips and Dudik 2008). Correlation between the 19 environmental variables from the WORLDCLIM database (1 km^2 resolution; Hijmans *et al.* 2005) was calculated with ENMtools v1.4.1 (Warren *et al.* 2010). Then, 9 environmental variables (correlation = $r \leq 0.80$) and presence points confirmed with molecular data (Appendix 1) were employed to obtain the ENMs. For clades I-III, 10 bootstrap replicates of presence/background points assigning 15 % of the presence points for training were applied. For clade IV, 10-fold cross-validation replicates were applied because of the limited number of presence records.

To test the hypothesis of niche conservatism between the ENMs from sister clades, a null distribution of 99 estimates of the I Statistics (Warren *et al.* 2008) and the Schoener's D (Schoener 1968) measures of niche overlap was generated for each pair of sister clades with the R package DISMO (Hijmans *et al.* 2017). In addition, a canonical discriminant function (CF) analysis was executed with the package candisc (Friendly and Fox 2015), to distinguish the potential affecting the extent to which their niches have been conserved. For this analysis, current time ENMs were reclassified so that each pixel predicted by each model would equal 1 and the rest of the grid 0. The resultant ENM masks were used to extract for each clade pixel-level data for the 9 environmental variables.

Lineage dispersal. To reconstruct the spatiotemporal history of lineage dispersal in *R. sumichrasti* we used the Relaxed Random Walk model (RRW; Lemey *et al.* 2010) as implemented in BEAST2. This model assumes an uncorrelated diffusion rate across the tree and infers the dispersal lineage history in space and time simultaneously, using both the phylogenetic tree and the geographic locations of the samples (Dellicour *et al.* 2021). To build the RRW we employed the geographic coordinates from each terminal collecting locality as a two-dimensional trait. We assumed a relaxed molecular clock (prior rate = 0.017, *SD* = 1.0), and the tree priors were calibrated as described above. To visualize the estimated phylogeographic reconstruction, space-time dispersal networks were created using SPREAD 1.0.6 (Bielejec *et al.* 2011).

Results

Phylogenetic hypothesis and species delimitation. The bGMYC species delimitation analysis of the Cyt-b recovered two species-level clades within *R. sumichrasti* ($P \geq 0.95$), separated by the Isthmus of Tehuantepec (Figure 3; Hypothesis 1). In this phylogeny, samples from new populations 64 to 66 from Guerrero and Oaxaca formed part of clade II. For the BPP and STACEY multiple-loci methods, the highest probability values (BPP, $pP = 0.56$; STACEY, $pP = 0.91$) supported Hypothesis five which recovered four divergent clades at the species level (Figure 3). One of them (clade I) was confined to the east and south of the Isthmus of Tehuantepec in México and Central America and the other three (clades II, III, and IV) were restricted to México. The K2P genetic distance values ranged from 5.43 % to 7.52 %, with the lowest value between clades II and IV and the highest between clades I and IV (Table 1). Similar genetic distance values among clades were obtained with the uncorrected *P*-distances (Table 1).

Table 1. Matrix of mean genetic distances (%) for Cytochrome b gene sequence data among the 4 clades delimited in *Reithrodontomys sumichrasti*. Values above (uncorrected *P*-distances) and below (Kimura 2-parameter) the diagonal represent genetic distances between clades. Numbers on the diagonal represent Kimura 2-parameter genetic distances within a clade.

R. sumichrasti	**Clade I**	**Clade II**	**Clado III**	**Clado IV**
Clade I	1.71	6.69	6.97	7.01
Clade II	7.16	1.66	5.74	5.17
Clade III	7.47	6.07	1.59	6.28
Clade IV	7.52	5.43	6.67	0.25

The species delimitation methods and the species tree (Figure 4) recovered the ancestral position of clade I ($pP = 0.84$), with a mean divergence time for the most recent common ancestor (MRCA) of ~2.15 Ma. The bGMYC supported the sister relationship between clades II and IV, whereas the multi-loci methods and the species tree supported the split of clade IV ($pP = 0.79$; mean divergence time 1.42 Ma), and a sister relationship between clades II and III ($pP = 0.70$; mean divergence time 0.90 Ma). In addition, the ancestral position of *R. chrysopsis* with respect to *R. megalotis-R. zacatecae* and *R. sumichrasti* was strongly supported ($pP = 1.00$), with an MRCA mean age estimated at 6.18 Ma. Also, a closer relationship was recovered between *R. humulis* and *R. montanus-R. raviventris* ($pP = 1.00$; mean divergence time 6.43 Ma), although the sister relationship of *R. montanus-R. ravivientris* received lower probabilities ($pP = 0.86$; mean divergence time 4.44 Ma).

Ecological niche equivalence. Ecological Niche Models generated for the four species-level clades within *R. sumichrasti* had AUC values above 0.90 for training data. The inter-clade predictability of the ENM of clade I ranged from 95 % when predicting known localities from clade III to 100 % when predicting known localities of clade IV (Figure 5). Clade IV had the most restricted ENM, and its inter-clade predictability ranged from 0 % when predicting clade III (and vice versa), to 18 % when predicting clade II. The ENMs of clades II and III showed the lowest intra-clade predictability values with 90 % and 95 %, respectively. Quantification of niche overlap with the I and Schoener's D statistics (from here forward *I* and *D*) revealed small amounts of overlap between each clade pair. For all clade pairwise comparisons, the niche identity (niche equivalency) hypothesis was rejected regardless of the similarity measure (*I* or *D*; Table 2).

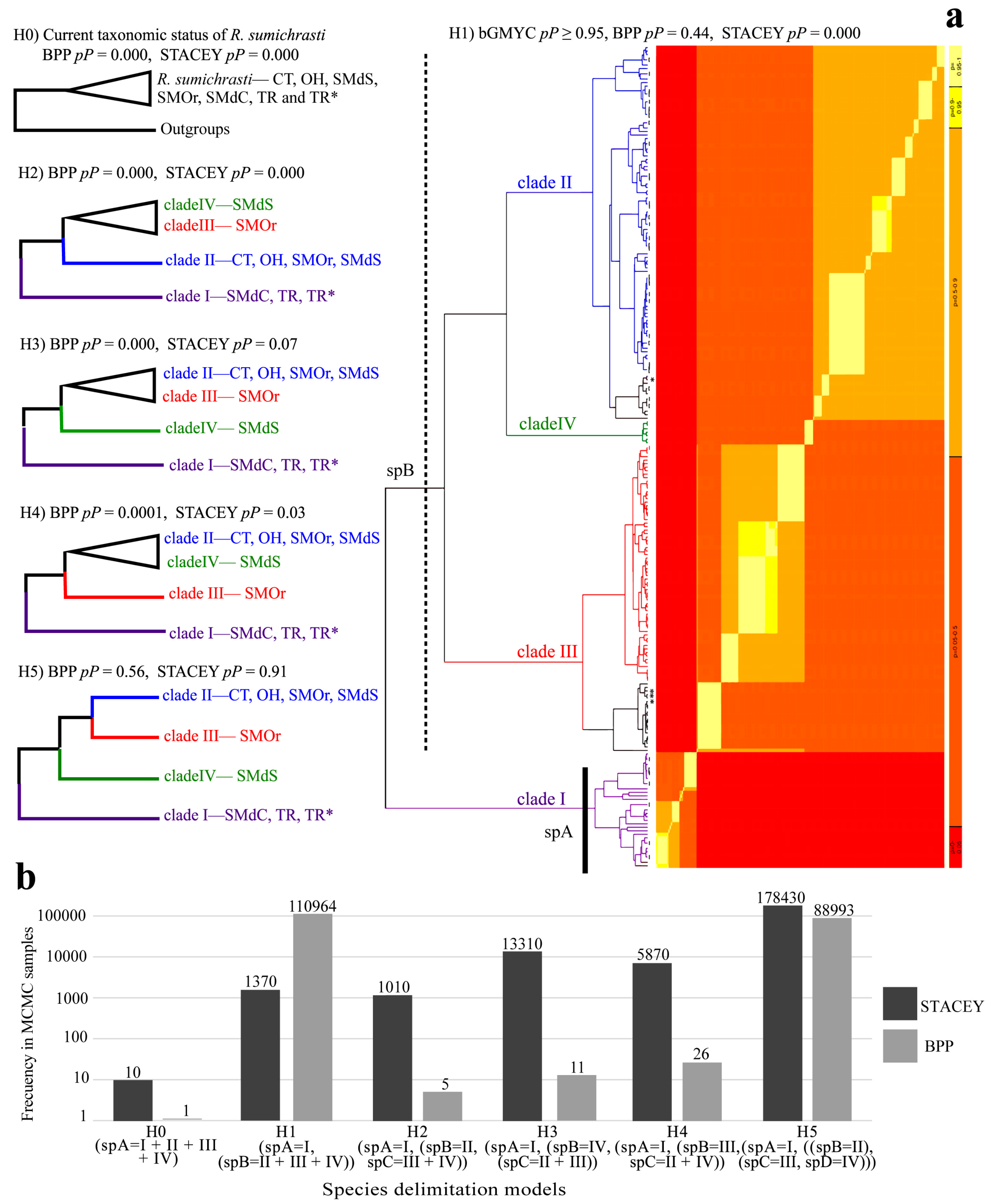

Figure 3. a) Single locus [Hypothesis 1; discontinuous red-yellow heat-map represents the *pP* ≥ 0.95 of belonging to different species (red color)] and multiple-loci (Hypothesis 2-Hypothesis 5) species delimitation models for *Reithrodontomys sumichrasti*. Solid and dashed lines denote the species delimitation proposal supported by bGMYC (Hypothesis 1; spA and spB). b) Amount of support for each model in the posterior sample (MCMC) of trees estimated with STACEY and BPP. The abbreviations of the physiographic provinces and clade colors follow Figure 2.

Table 2. Niche comparisons between sister clades of *Reithrodontomys sumichrasti*. The I statistics and Schoener's D represent the observed niche overlap values and the Identity tests represent the comparison of niche equivalency between each clade.

R. sumichrasti	**Clade**	**Schoener's D**	**I statistics**	**Identity test**
Clade I	II	0.1322	0.3075	niche non-equivalency
	III	0.4369	0.7547	niche non-equivalency
	IV	0.2722	0.5371	niche non-equivalency
Clade II	III	0.3803	0.6456	niche non-equivalency
	IV	0.1872	0.3900	niche non-equivalency
Clade III	IV	0.0260	0.0843	niche non-equivalency

The canonical variable analysis did not discriminate significantly among the ENMs of the clades (Figure 6). The first and second canonical functions accounted for 97.3 % of the variance and the meaningful structure coefficients (> 0.3) were exclusively related to temperature (BIO1, BIO2, BIO4, BIO5, BIO6, BIO7). Overall, there was more similarity among mean values of each climatic variable between the ENM of clades II and III, whereas the area that occupied clade IV displayed extreme values for the Max Temperature of Warmest Month (BIO5; 27.4 °C), Annual Precipitation (BIO12; 1086 mm), and Precipitation of Driest Quarter (BIO17; 14.86 mm; Table 3).

Lineage dispersal. The RRW model predicted the ancestral distribution of *R. sumichrasti* was centered in the SMdC physiographic region (abbreviations described in Figure 2), within the current extent of clade I (Figure 7). This clade started to spread at ~1.80 - 1.75 Ma to the west crossing the Tehuantepec Isthmus towards both the Oaxacan Highlands (OH) and Sierra Madre del Sur (SMdS) where the MRCA of clades II, III, and IV originated. Subsequently (between 1.53 - 1.25 Ma), the MRCA of clade III extended to the Sierra Madre Oriental (SMOr), while clade I colonized the Costa Rican Seasonal Moist Forest (TR*) and Talamancan Range (TR) regions. By ~1.25 to 0.65 Ma, the ancestor of clade IV expanded to the west of the Mexican Transvolcanic Belt

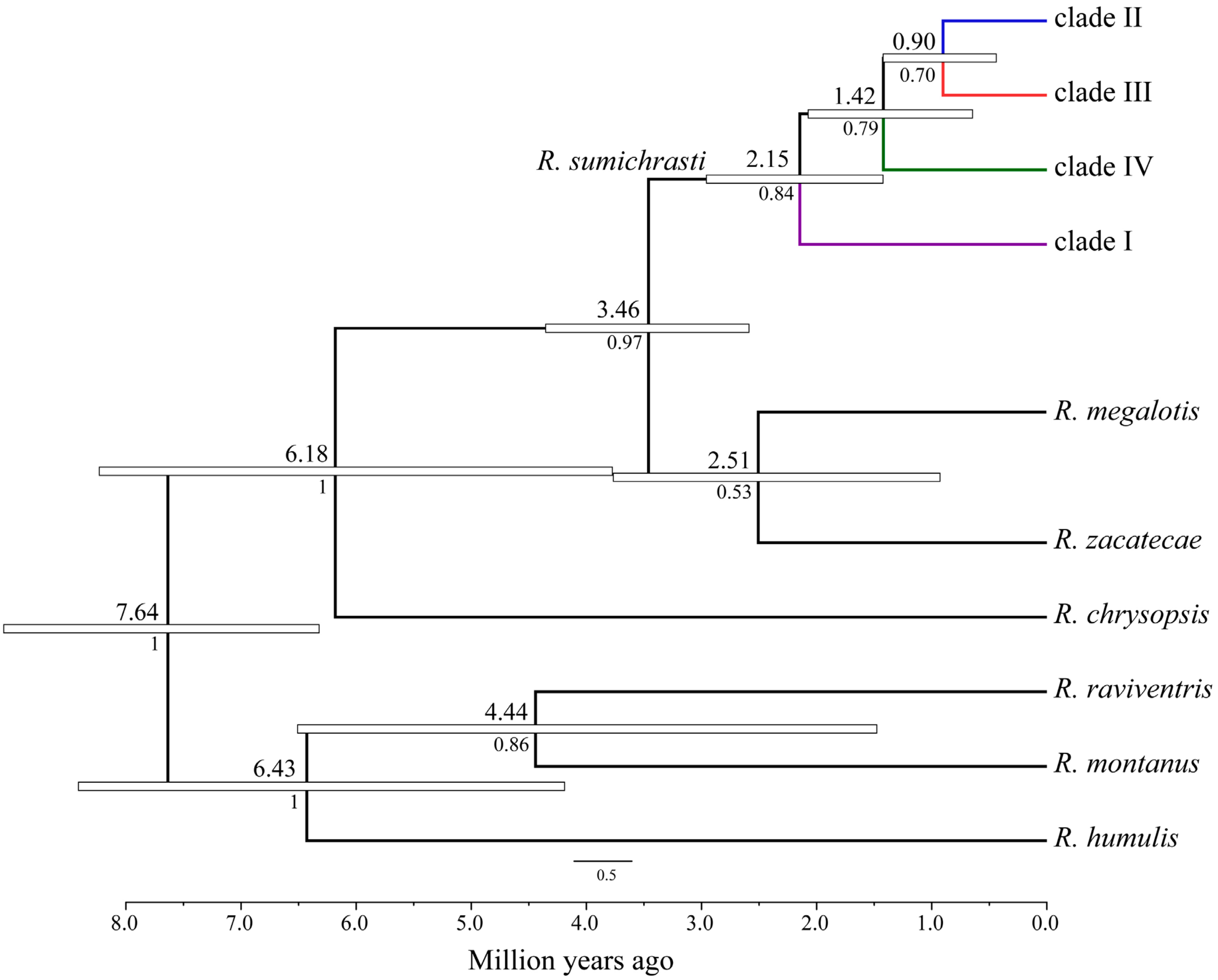

Figure 4. Time-calibrated species tree estimated with *BEAST-STACEY for *Reithrodontomys sumichrasti* and the outgroup taxa. Values above branches indicate the mean divergence times (millions of years) and below are the Bayesian posterior probabilities for clades. White bars represent the 95% highest posterior density intervals. Colors follow the clade-color distinction described in Figure 2. Specimens assigned to the collapsed terminal taxa are listed in Appendix 1.

(CT as named in Hardy *et al.* 2013), and by ~ 0.11 Ma most dispersal events occurred when clade II expanded through the central and east of the CT, but also seemed to expand towards the east by the OH (Figure 7).

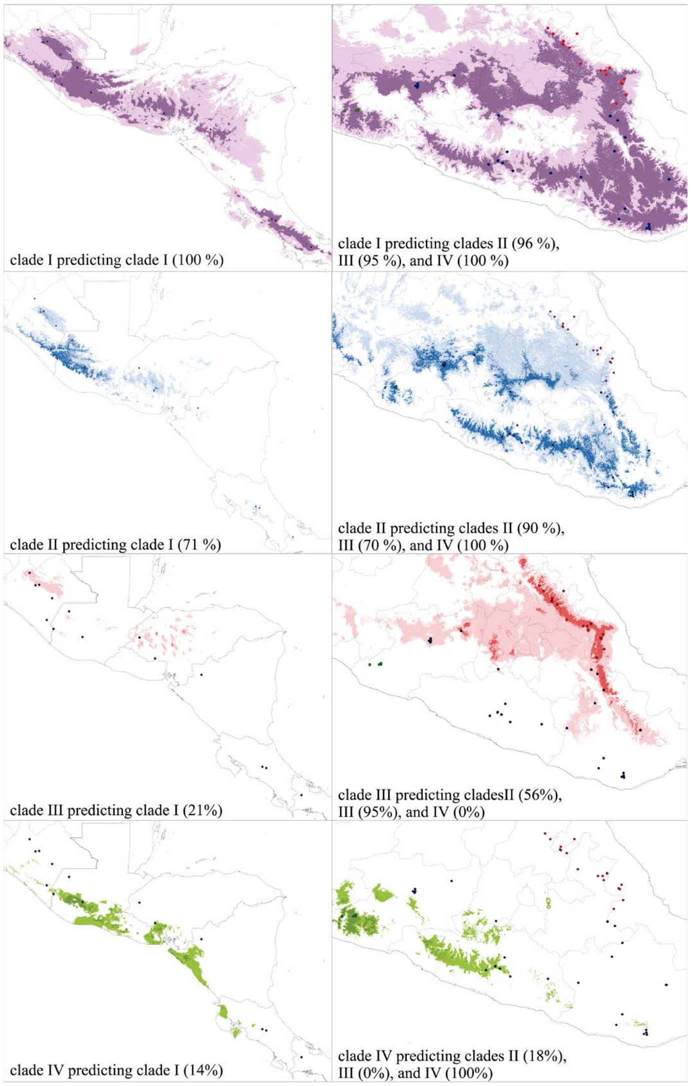

Figure 5. Map projection of the Ecological Niche Models for the 4 clades of *Reithrodontomys sumichrasti* indicating the within-clade and inter-clade localities predictability values. Color dots represent the presence records of each clade and follow the clade-colors in Figure 2. Dark and light colors on the maps represent the suitable and non-suitable areas of each clade, respectively.

Discussion

Species delimitation. The use of innovative tools and methodologies to assess species boundaries has helped to clarify taxonomic problems while facilitating the generation of robust hypotheses to reveal cryptic species and describe the speciation processes (Dayrat *et al.* 2005; Padial *et al.* 2010). Such is the case of mammals distributed in Mesoamerica, characterized by a peculiar evolutionary history that is linked to the environmental and biogeographical characteristics of this region (see Almendra and Rogers 2012). We used the cricetid rodent *R. sumichrasti* because it is a good model to evaluate the biogeographical and ecological niche conservatism hypotheses linked to vicariant speciation events in México to Central America. This approach was addressed by other authors (Sullivan *et al.* 2000; Martínez-Gordillo *et al.* 2010; Hardy *et al.* 2013), but this is the first time that the use of mathematical methods for species delimitation and phylogeographic reconstruction is put into practice for this species.

Our results show that the species delimitation methods support the phylogenetic hypotheses one and five with higher posterior probabilities, suggesting that *R. sumichrasti* is a complex of multiple species. In both hypotheses, clade I was identified as a distinct species, as this result was congruent among the three species delimitation methods. Recognition of clade I at the species level has been suggested previously due to its position in the molecular phylogenies (Sullivan *et al.* 2000; Hardy *et al.* 2013), and to the *P*-distances to the remaining clades (6.15 % to 9.10 %; Hardy *et al.* 2013). We agree with this species-level suggestion since this clade was placed as an independent sister lineage to the other clades of *R. sumichrasti* in our phyloge-

Table 3. Coefficients of the three first canonical discriminant functions derived from the bioclimatic variables used in the ecological analyses in *Reithrodontomys sumichrasti*. Mean values of the bioclimatic variables based on the environmental information from occurrence records are given for each clade.

Climatic Variable	Function 1 Eigen=0.261	Function 2 Eigen=0.035	Function 3 Eigen=0.008	Clade I	Clade II	Clade III	Clade IV
BIO1	0.689	0.402	0.028	17.11	16.75	14.15	18.44
BIO2	-0.054	0.409	0.023	11.82	12.23	12.18	12.96
BIO4	0.632	0.086	0.021	104.09	124.54	185.44	164.25
BIO5	0.239	0.486	0.379	24.88	25.24	23.17	27.47
BIO6	-0.385	0.280	0.252	9.00	8.16	4.40	8.30
BIO7	-0.614	0.671	0.015	15.88	17.09	18.77	19.17
BIO11	0.421	0.149	0.619	15.70	15.11	11.64	16.16
BIO12	-0.257	0.116	0.056	1723.79	1237.19	1157.14	1086
BIO17	-0.196	0.232	0.302	79.52	34.47	98.99	14.86
EV (%)	85.575	11.724	2.700				

BIO1 = Annual Mean Temperature; BIO2 = Mean Diurnal Range (Mean of monthly (max temp - min temp)); BIO4 = Temperature Seasonality (standard deviation *100); BIO5 = Max Temperature of Warmest Month; BIO6 = Min Temperature of Coldest Month, BIO7 = Temperature Annual Range (BIO5-BIO6); BIO11 = Mean Temperature of Coldest Quarter; BIO12 = Annual Precipitation; BIO17 = Precipitation of Driest Quarter; EV (%) = Percent of explained variance.

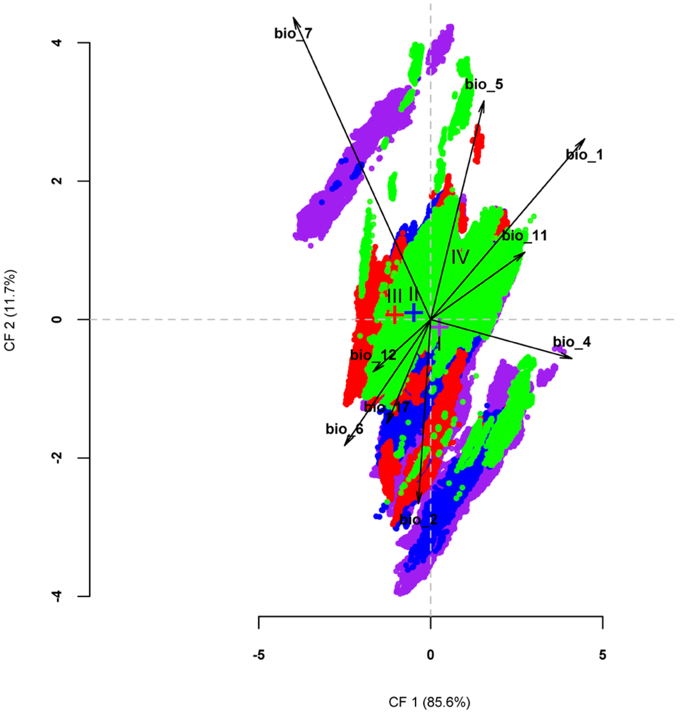

Figure 6. Graphic of the first two discriminant functions among Ecological Niche Models of clades I to IV of *Reithrodontomys sumichrasti*. Colored crosses represent the centroid of each clade environmental niche. Colors follow the clade-color distinction described in Figure 2. Black arrows denote the power and direction of the discrimination for that bioclimatic variable (see text and Table 3 for descriptions of bioclimatic variables).

netic trees and also showed the highest genetic divergence (both K2P and *P*-distances) compared to clades II-IV. The populations belonging to this clade are distributed southeast of the Isthmus of Tehuantepec, from the Sierra Madre de Chiapas, México to western Panama (Hall 1981), and were the first to diverge from a common ancestor ~2.15 Ma. This mean age is close to that reported by Hardy *et al* (2013; ~2.56 Ma), placing the species diversification within *R. sumichrasti* at the Plio-Pleistocene boundary (see discussion below).

The proposal that clade I evolved independently was better supported by molecular data than by ecological data. The environmental niche space that this clade occupies predicted the potential distribution areas of the remaining clades with high percentages, although the inverse was not true. In general, *R. sumichrasti sensu lato* inhabits brush and grass in pine-oak and cloud forests throughout its geographical distribution. However, Hooper (1952) reported a greater diversity of habitats for the subspecies that encompass clade I, particularly for *R. s. dorsalis* and *R. s. australis*. This apparently broad environmental range could explain the high percentages of predictability we found, which was also evidenced in the canonical analysis. Nevertheless, non-equivalency of niche was found in the niche identity test. The remaining ecological analyses showed a relatively high similarity between this clade and clades II-IV, suggesting that their differentiation at the species level within *R. sumichrasti sensu lato* was more favored by geography than by ecology (Peterson *et al.* 1999).

The species delimitation methods were not consistent in the delimitation of clades II, III, and IV. The single-locus bGMYC (Cyt-b) proposed that the three clades form a single species, while the multiple-loci BPP and STACEY (Cyt-b + Fgb-I7 + Acp5) considered each clade as a distinct species. Molecular delimitation methods are considered a valuable complement to taxonomy based on morphological traits and are often used as part of an integrative approach to validate putative species (Luo *et al.* 2018). The three delimitation methods used in our study have been recognized for their high performance for this purpose (Jones 2017; Luo *et al.* 2018), but only two of them (BPP and STACEY) were consistent in this work. The performance and accuracy of each method can be affected by factors including both biological (variation in population size, uninterrupted gene flow) and methodological (input tree), among others, so they can over or underestimate the number of species (Rannala 2015; Luo *et al.* 2018). For this reason, the use of different molecular delimitation methods is highly recommended with species hypotheses based on the congruence among them (Carstens *et al.* 2013). In accordance with this suggestion, Hypothesis five (which is based on multiple loci) should be accepted and therefore each clade distributed west of the Isthmus of Tehuantepec constitutes a distinct species-level entity. Hypothesis five (Fig. 2) was also supported by the amount of Cyt-b genetic differentiation among clades. The K2P genetic distance values between pairwise clades II-III, II-IV, and III-IV were 6.07, 5.43, and 6.67, respectively, which are greater than the 5 % value associated with sister species recognition in mammals (Baker and Bradley 2006) including rodents (ranged from 2.70 % to 19.23 %; Bradley and Baker 2001).

Phylogenetic relationships among clades II, III, and IV were different between the Cyt-b tree topology and the species tree, but generally with weak nodal support. In the first case, II and IV were recovered as sister clades, while in the second, clades II and III were more closely related. These results partially coincide with the topologies obtained by Hardy *et al.* (2013), in which their concatenated DNA tree is consistent with our species tree. On the other hand, none of our phylogenies (gene tree or species tree) recovered sister relationships between clades III and IV, such as those obtained in the Cyt-b tree of Hardy *et al.* (2013). This is also supported by the ecological results where there is a greater ecological similarity (based on both directions of area predictability) between clades II and III than between clades II and IV or III and IV.

The ecological niche characteristics (from the bioclimatic variables used) of clade II showed high predictability percentages of the ecological suitability areas of clades III and IV, but these tended to have low or null values when the inverse analysis was performed. For example, clade IV predicted only 18 % of clade II and 0 % of clade III. The geographical distribution of each clade could explain the different percentages of predictability of the environmental niche. The wide geographical distribution of clade II

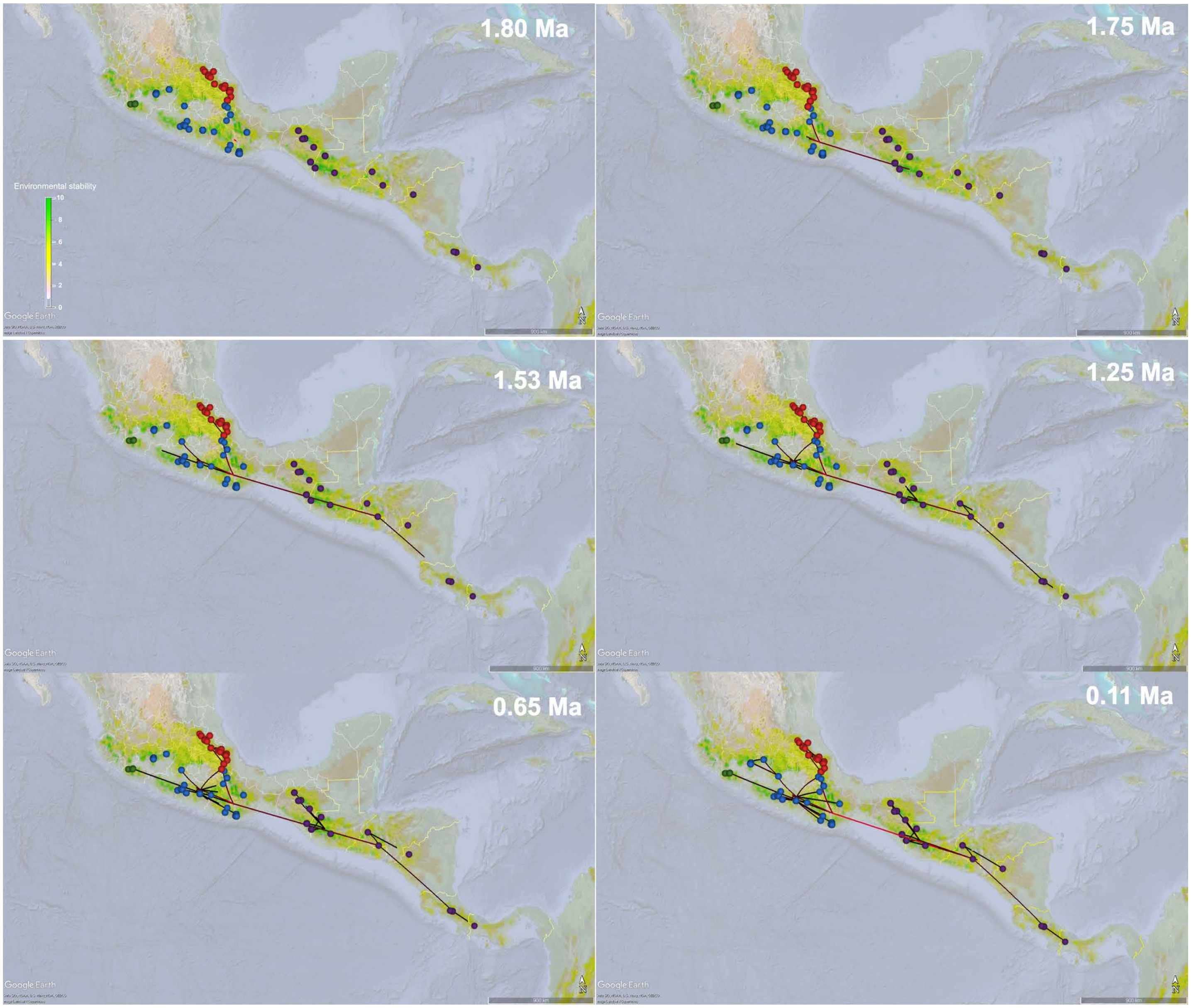

Figure 7. Spatiotemporal dynamics of the *Reithrodontomys sumichrasti* lineages diffusion for 1.80 Ma, 1.75 Ma, 1.53 Ma; 1.25 Ma, 0.65 Ma, and 0.11 Ma. Lines represent the branches of the Maximum Clade Credibility Tree and circles the location of occurrence records of the terminal labels (Appendix 1). An overlay of the sum of current, Last Glacial Maximum, and Last Interglacial ENMs was added to denote areas of relative environmental stability. Line and circle colors follow the clade-color distinction described in Figure 2. Maps were generated using Google Earth (http://earth.google.com).

includes localities of the CT, SMdS, extreme south of SMOr, and OH, while clade III is distributed in the SMOr, and clade IV is restricted to Coalcomán and Dos Aguas localities, in Michoacán (Hall 1981; Hardy *et al.* 2013; Figure 1, 2).

Niche pairwise comparisons showed low observed values for *D* and *I* similarity indices, mainly between clades III and IV. This is based on the fact that these indices can take values from 0 (no niche overlap) to 1 (total niche overlap; Warren *et al.* 2008). Closely related species are predicted to share characteristics of their environmental niche due to their common ancestry (Peterson *et al.* 1999), but niche differentiation can occur when allopatric populations exist, and gene flow is assumed to have been disrupted in the past (Avise 2000; Martínez-Gordillo *et al.* 2010). This could explain the non-equivalency of niche between these clades, as well as the low values of area predictability, which coincides with reports of Martínez-Gordillo *et al.* (2010) for different rodent species, including *R. sumichrasti*.

Bioclimatic data show that clade II shared similar characteristics to the other clades depending on the variable being analyzed. Moreover, clade III was characterized by low temperatures and the second-highest value of annual mean precipitation. These bioclimatic characteristics correspond to the habitat description of *R. s. sumichrasti*, mainly associated with pine and pine-oak forests, in "areas frequently bathed by clouds and rain (Hooper 1952:72)". In contrast, clade IV was associated with higher temperatures and lower precipitation values, showing extreme values with respect to the other clades in at least five of the nine variables analyzed. Hardy *et al.* (2013) highlighted the presence of geographical barriers such as low-lying river drainages that have isolated clade IV populations from other *R. sumichrasti sensu lato* populations, which could justify our molecular and ecological results regarding the species recognition of this clade.

Phylogeographic history. Our results suggest that the common ancestor of the *R. sumichrasti sensu lato* originated in the montane regions of northern Central America ~2 Ma ago and expanded to where this species complex currently occurs. Various geographic and environmental factors may have favored and/or limited its dispersal in Central America and México (for more details see Hardy *et al.* 2013). The montane and intermontane Central America regions have a deep tectonic and volcanic history, which may have influenced the origin and diversification of montane species such as *Peromyscus guatemalensis*, *P. bakeri*, and *P. carolpattonae* (Álvarez-Castañeda *et al.* 2019). Also, the Pleistocene glacial cycles may have played a key role, due to favorable climatic conditions (Ceballos *et al.* 2010), which allowed the colonization of new areas and in some cases new habitats, followed by post-glacial isolation that limited the gene flow between populations (Martin 1961). This has been reported in several groups such as plants (*e. g.* Ramírez-Barahona and Eguiarte 2013), reptiles and amphibians (*e. g.* Church *et al.* 2003; Howes *et al.* 2006), birds (*e. g.* Johnson and Cicero 2004; Baker 2008), and mammals (*e. g.* Ceballos *et al.* 2010; Chiou *et al.* 2011) including other species of *Reithrodontomys* (Martínez-Borrego *et al.* 2022). In addition, geographic regions such as the Isthmus of Tehuantepec seem to have acted as an efficient barrier limiting gene flow between populations that are distributed on both sides of the Isthmus, an accepted explanation for *R. sumichrasti* and other rodent species (*e. g.* Sullivan *et al.* 2000; León-Paniagua *et al.* 2007; Ordoñez-Garza *et al.* 2010; Hardy *et al.* 2013).

The lineage dispersal in México was from populations in the west of the OH and SMdS that currently belong to the clade II, which spread into SMOr (clade III) and the west of CT (clade IV) as well as through the central and east of the CT (clade II). This model would explain the wide geographical distribution of clade II, and also its greater number of haplotypes compared to the other clades (Hardy *et al.* 2013). Although these dispersal events seem to have occurred relatively recently, the physiographic characteristics of the Mexican mountainous regions (Morrone 2005; Escalante *et al.* 2009) could have favored relatively faster speciation processes within *R. sumichrasti* complex, leading to differentiation, at least genetically and ecologically, among each clade analyzed here. This seems to be a common pattern in several species of small mammals, where the allopatric effect and the habitat characteristics each ancestral species occupied resulted in complete speciation of lineages, often associated with cryptic speciation processes (*e. g.* Arellano *et al.* 2005; Rogers *et al.* 2007; León-Tapia *et al.* 2021; Martínez-Borrego *et al.* 2022).

Taxonomic considerations. Species delimitation methods and values of genetic divergence support the recognition of populations of *R. sumichrasti* at the east and south of the Isthmus of Tehuantepec, from Chiapas, México to Central America (Clade I), as a valid species which is different from everything occurring to the west of this geographical barrier. According to this hypothesis, then *R. australis* (Allen 1895) is the taxonomic name that has priority (Article 23; ICZN 1999). Subspecies distributed across this region of Mesoamerica, beyond the nominotypical would include *R. a. dorsalis* (Merriam 1901), *R. a. modestus* (Thomas 1907), and *R. a. vulcanius* (Bangs 1902).

In addition, the existence of an undescribed species represented by the populations included in clade IV, from Coalcomán and Dos Aguas in Michoacán, México (northwestern SMdS) is supported by species delimitation methods and values of genetic divergence. The disjoint distribution of this genetically distinct clade suggests that it does not belong to *R. s. nerterus* nor *R. s. luteolus*. The mountainous region inhabited by this new species is isolated from other mountain ranges in the area by lowlands of up to approximately 400 masl. This pattern of genetic differentiation coincides with the recent description of a new species of the genus *Peromyscus* (*P. greenbaumi*; Bradley *et al*. 2022; but see also León-Tapia *et al.* 2021). In order to make the formal description based on diagnostic characters that will derive in an appropriate species name, a morphological comparison would be necessary.

Molecular species delimitation and genetic distance values associated to populations from clades II and III indicate that these two lineages should be recognized as valid species. Nomenclatural suggestions are difficult to make due to the sympatry of individuals of some populations from both clades. This was already addressed by Hardy *et al.* (2013) through nested clade analysis. In our study a phylogeographic pattern of diffusion of the lineages (RRW model) suggests colonization after the separation of clades II and III. Nevertheless, in this work we propose populations comprising clade II should be recognized as *R. nerterus* (Merriam, 1901). Although we did not include specimens from the type locality of *R. nerterus* (El Nevado de Colima, Jalisco, México), we analyzed several individuals from sites reported by Hooper (1952) for this taxon. Because clade II includes populations of the known distribution of *R. s. luteolus*, this taxon should be considered as subspecies of *R. nerterus*. Clade III should be named as *R. sumichrasti*; here we also did not include individuals from the type locality (El Mirador, Veracruz, México), but we used specimens from localities that belong to this species. Populations from south Puebla and Northern Oaxaca (28, 1, and 10 in Figure 2), regarded originally as *R. s. sumichrasti* should be now *R. n. luteolus*. It remains necessary to evaluate sympatric populations from both clades in order to identify plausible evolutionary processes in this region.

Acknowledgements

We acknowledge financial support from the Consejo Nacional de Ciencia y Tecnologia (postdoctoral fellowship to ALA) and the Department of Biology, Brigham Young University (to DSR). We wish to thank D. D. Cruz for his assistance in compiling data for the Ecological Niche Modeling, E. C. Molina for gathering GeneBank data for the molecular analysis, and R. Núñez for his support in editing figures. We also thank two anonymous reviewers who kindly read drafts of this work and supplied valuable comments.

Literature cited

Allen, J. A. 1895. On the species of the genus *Reithrodontomys*. Bulletin of the American Museum of Natural History 7:7-143.

Almendra, A. L., and D. S. Rogers. 2012. Biogeography of Central American mammals. Pp. 203-229, *in* Bones, clones, and biomes: the history and geography of recent neotropical mammals (Patterson, B. D., and L. P. Costa, eds.). University of Chicago Press. Illinois, U.S.A.

Almendra, A. L., *et al*. 2018. Evolutionary relationships and climatic niche evolution in the genus *Handleyomys* (Sigmodontinae: Oryzomyini). Molecular Phylogenetics and Evolution 128:12-25.

Álvarez-Castañeda, S. T., *et al*. 2019. Two new species of *Peromyscus* from Chiapas, Mexico, and Guatemala. Pp. 543-558, *in* From field to laboratory: a memorial volume in honor of Robert J. Baker (Bradley, R. D., H. H. Genoways, D. J. Schmidly, and L. C. Bradley, eds.). Special Publications, Museum of Texas Tech University. Lubbock, U.S.A.

Arbogast, B. S., *et al*. 2002. Estimating divergence times from molecular data on phylogenetic and population genetic timescales. Annual Review of Ecology and Systematics 33:707-740.

Arellano, E., F. González-Cozátl, and D. S. Rogers. 2005. Molecular systematics of Middle American harvest mice *Reithrodontomys* (Muridae), estimated from mitochondrial cytochrome b gene sequences. Molecular Phylogenetics and Evolution 37:529-540.

Avise, J. C. 2000. Phylogeography: the history and formation of species. Harvard University Press. Massachusetts, U.S.A.

Baker, A. J. 2008. Islands in the sky: the impact of Pleistocene climate cycles on biodiversity. Journal of Biology 7:1-4.

Baker, R. J., and R. D. Bradley. 2006. Speciation in mammals and the Genetic Species Concept. Journal of Mammalogy 87:643-662.

Bangs, O. 1902. Chiriqui Mammalia. Bulletin of the Museum of Comparative Zoology at Harvard College 39:17-51.

Bielejec, F., *et al*. 2011. SPREAD: spatial phylogenetic reconstruction of evolutionary dynamics. Bioinformatics 27:2910-2912.

Bouckaert, R., *et al*. 2014. BEAST 2: a software platform for Bayesian evolutionary analysis. PLoS Computational Biology 10:p.e1003537.

Bradley, R. D. 2017. Genus *Reithrodontomys*. Pp. 367-383, *in* Handbook of the Mammals of the World: Rodents II (Wilson, D. E., T. E. Lacher, and R. A. Mittermeier, eds.). Lynx Edicions. Barcelona, Spain.

Bradley, R. D., and R. J. Baker. 2001. A test of the Genetic Species Concept: Cytochrome *b* sequences and mammals. Journal of Mammalogy 82:960-973.

Bradley, R. D., *et al*. 2022. Two new species of *Peromyscus* (Cricetidae: Neotominae) from the Transverse volcanic belt of Mexico. Journal of Mammalogy 103:255-274.

Carstens, B. C., *et al*. 2013. How to fail at species delimitation. Molecular Ecology 22:4369-4383.

Ceballos, G., J. Arroyo-Cabrales, and E. Ponce. 2010. Effects of Pleistocene environmental changes on the distribution and community structure of the mammalian fauna of Mexico. Quaternary Research 73:464-473.

Chiou, K. L., *et al*. 2011. Pleistocene diversification of living squirrel monkeys (*Saimiri* spp.) inferred from complete mitochondrial genome sequences. Molecular Phylogenetics and Evolution 59:736-745.

Church, S. A., *et al*. 2003. Evidence for multiple Pleistocene refugia in the postglacial expansion of the eastern tiger salamander, *Ambystoma tigrinum tigrinum*. Evolution 57:372-383.

Czaplewski, N. J. 1987. Sigmodont rodents (Mammalia; Muroidea; Sigmodontinae) from the Pliocene (early Blancan) Verde Formation, Arizona. Journal of Vertebrate Paleontology 7:183-99.

Dalquest, W. W. 1978. Early Blancan mammals of the Beck Ranch local fauna of Texas. Journal of Mammalogy 59:269-98.

Daly, M., *et al*. 2012. Systematics Agenda 2020: the mission evolves. Systematic Biology 61:549-552.

Dayrat, B. 2005. Towards integrative taxonomy. Biological Journal of Linnean Society 85:407-415.

de Queiroz, K. 2007. Species concepts and species delimitation. Systematic Biology 56:879-886.

Dellicour, S., *et al*. 2021. Relax, keep walking—a practical guide to continuous phylogeographic inference with BEAST. Molecular Biology and Evolution 38:3486-3493.

Doody, J. S., S. Freedberg, and J. S. Keogh. 2009. Communal egg-laying in reptiles and amphibians: evolutionary patterns and hypotheses. The Quarterly Review of Biology 84:229-252.

Escalante, T., C. Szumik, and J. J. Morrone. 2009. Areas of endemism of Mexican mammals: reanalysis applying the optimality criterion. Biological Journal of the Linnean Society 98:468-478.

Friendly, M., and J. Fox. 2015. candisc: Visualizing generalized canonical discriminant and canonical correlation analysis. R package version 0.6-5. Available from: https://cran.r-project.org/web/packages/candisc/index.html

Gilbert, J. D., and A. Manica. 2015. The evolution of parental care in insects: a test of current hypotheses. Evolution 69:1255-1270.

Hall, E. R. 1981. The Mammals of North America 2nd ed. John Wiley and Sons, Inc., New York, U.S.A.

Hardy, D. K., *et al*. 2013. Molecular phylogenetics and phylogeography structure of Sumichrast´s harvest mouse (*Reithrodontomys sumichrasti*: Cricetidae) based on mitochondrial and nuclear DNA sequences. Molecular Phylogenetics and Evolution 68:282-292.

Heath, T. A., J. P. Huelsenbeck, and T. Stadler. 2014. The fossilized birth-death process for coherent calibration of divergence-time estimates. Proceedings of the National Academy of Sciences 111:2957-2966.

Heled, J., and A. J. Drummond. 2010. Bayesian inference of species trees from multilocus data. Molecular Biology and Evolution 27:570-580.

Hijmans, R. J., *et al*. 2005. Very high-resolution interpolated climate surfaces for global land areas. International Journal of Climatology 25:1965-1978.

Hijmans, R. J., *et al*. 2017. Package 'dismo'. Circles 9:1-68.

Hooper, E. T. 1952. A systematic review of harvest mice (genus *Reithrodontomys*) of Latin America. Miscellaneous Publications Museum of Zoology, University of Michigan 77:1-255.

Howes, B. J., B. Lindsay, and S. C. Lougheed. 2006. Range-wide phylogeography of a temperate lizard, the five-lined skink (*Eumeces fasciatus*). Molecular Phylogenetics and Evolution 40:183-194.

Huang, J. P. 2020. Is population subdivision different from speciation? From phylogeography to species delimitation. Ecology and Evolution 10:6890-6896.

International Commission on Zoological Nomenclature. 1999. International code of zoological nomenclature. 4th ed. International Trust for Zoological Nomenclature, London, U.K.

Johnson, N. K., and C. Cicero. 2004. New mitochondrial DNA data affirm the importance of Pleistocene speciation in North American birds. Evolution 58:1122-1130.

Jones, G. 2017. Algorithmic improvements to species delimitation and phylogeny estimation under the multispecies coalescent. Journal of Mathematical Biology 74:447-467.

Katoh, K., *et al*. 2005. MAFFT version 5: improvement in accuracy of multiple sequence alignment. Nucleic Acids Research 33:511-518.

Kimura, M. 1980. A simple method for estimating evolutionary rates of base substitutions through comparative studies of nucleotide sequences. Journal of Molecular Evolution 16:111-120.

Knowles, L. L., and B. C. Carstens. 2007. Delimiting species without monophyletic gene trees. Systematic Biology 56:887-895.

Kumar, S., *et al*. 2018. MEGA X: molecular evolutionary genetics analysis across computing platforms. Molecular Biology and Evolution 35:1547-1549.

Lanfear, R., *et al*. 2014. Selecting optimal partitioning schemes for phylogenomic datasets. BMC Evolutionary Biology 14:1-14.

Lemey, P., *et al*. 2010. Phylogeography takes a relaxed random walk in continuous space and time. Molecular Biology and Evolution 27:1877-1885.

León-Paniagua, L., *et al*. 2007. Diversification of the arboreal mice of the genus *Habromys* (Rodentia: Cricetidae: Neotominae) in the Mesoamerican highlands. Molecular Phylogenetics and Evolution 42:653-664.

León-Tapia, M. Á., *et al*. 2021. Role of Pleistocene climatic oscillations on genetic differentiation and evolutionary history of the Transvolcanic deer mouse *Peromyscus hylocetes* (Rodentia: Cricetidae) throughout the Mexican central highlands. Journal of Zoological Systematics and Evolutionary Research 59:2481-2499.

Lindsay, E. H., and N. J. Czaplewski. 2011. New rodents (Mammalia, Rodentia, Cricetidae) from the Verde Fauna of Arizona and the Maxum Fauna of California, USA, early Blancan Land Mammal Age. Palaeontología Electrónica 14:1-16.

Luo, A., *et al*. 2018. Comparison of methods for molecular species delimitation across a range of speciation scenarios. Systematic Biology 67:830-846.

Maestri, R., *et al*. 2017. The ecology of continental evolutionary radiation: Is the radiation of sigmodontine rodents adaptive? Evolution 71:610-632.

Martin, P. S. 1961. Southwestern animal communities in the late Pleistocene. Biology of the arid and semiarid lands of the Southwest. New Mexico Highlands University Bulletin 212:56-66.

Martin, R. A., *et al*. 2002. Blancan Lagomorphs and rodents of the Deer Park assemblages, Meade County, Kansas. Journal of Paleontology 76:1072-1090.

Martin, R. A., *et al*. 2003. Late Pliocene and early Pleistocene rodents from the northern Borchers Badlands (Meade County, Kansas), with comments on the Blancan-Irvingtonian boundary in the Meade Basin. Journal of Paleontology 77:985-1001.

Martin, R. A., and P. Peláez-Campomanes. 2014. Diversity dynamics of the Late Cenozoic rodent community from south-western Kansas: the influence of historical processes on community structure. Journal of Quaternary Science 29:221-231.

Martínez-Borrego, D., *et al*. 2022. Molecular systematics of the *Reithrodontomys tenuirostris* group (Rodentia: Cricetidae) highlighting the *Reithrodontomys microdon* species complex. Journal of Mammalogy 103:29-44.

Martínez-Gordillo, D., O. Rojas-Soto, and A. Espinosa-De Los Monteros. 2010. Ecological niche modelling as an exploratory tool for identifying species limits: an example based on Mexican muroid rodents. Journal of Evolutionary Biology 23:259-270.

Merriam, C. H. 1901. Descriptions of 23 new harvest mice (genus *Reithrodontomys*). Proceedings of the Washington Academy of Sciences 3:547-558.

Morgan, G. S, and R. S. White Jr. 2005. Miocene and Pliocene vertebrates from Arizona. Pp. 114-135, *in* Vertebrate Paleontology in Arizona (Heckert A. B. and S. G. Lucas, eds.). New Mexico Museum of Natural History and Science Bulletin. Albuquerque, New Mexico, U.S.A.

Morrone, J. J. 2005. Toward a synthesis of Mexican biogeography. Revista Mexicana de Biodiversidad 76:207-252.

Musser, G. G., and M. D. Carleton. 2005. Superfamily Muroidea. Pp. 894-1531, *in* Mammal species of the world: a taxonomic and geographic reference. 3rd ed. (D. E. Wilson and D. M. Reeder, eds.). Johns Hopkins University Press. Baltimore, U.S.A.

Myers, N., *et al*. 2000. Biodiversity hotspots for conservation priorities. Nature 403:853-858.

Ordóñez-Garza, N., *et al*. 2010. Patterns of phenotypic and genetic variation in three species of endemic Mesoamerican *Peromyscus* (Rodentia: Cricetidae). Journal of Mammalogy 91:848-859.

Padial, J., *et al*. 2010. The integrative future of taxonomy. Frontiers in Zoology 7:16.

Peterson, A. T., J. Soberón, and V. Sánchez-Cordero. 1999. Conservatism of ecological niches in evolutionary time. Science 285:1265-1267.

Phillips, S. J., and M. Dudík. 2008. Modeling of species distributions with Maxent: new extensions and a comprehensive evaluation. Ecography 31:161-175.

R Development Core Team. 2018. R: A language and environment for statistical computing. R Foundation for Statistical Computing. Vienna, Austria. www.R-project.org/

Rambaut, A., *et al*. 2018. Posterior summarization in Bayesian phylogenetics using Tracer 1.7. Systematic Biology 67:901-904.

Ramírez-Barahona, S. and L. E. Eguiarte. 2013. The role of glacial cycles in promoting genetic diversity in the Neotropics: the case of cloud forests during the Last Glacial Maximum. Ecology and Evolution 3:725-738.

Rannala, B. 2015. The art and science of species delimitation. Current Zoology 61:846-853.

Reid, N. M., and B. C. Carstens. 2012. Phylogenetic estimation error can decrease the accuracy species delimitation: a Bayesian implementation of the General Mixed Yule Coalescent model. BMC Evolutionary Biology 12:196.

Rissler, L. J., and J. J. Apodaca. 2007. Adding more ecology into species delimitation: ecological niche models and phylogeography help define cryptic species in the black salamander (*Aneides flavipunctatus*). Systematic Biology 56:924-942.

Rogers, D. S., *et al*. 2007. Molecular phylogenetic relationships among crested-tailed mice (genus *Habromys*). Journal of Mammalian Evolution 14:37-55.

Sites Jr., J. W., and J. C. Marshall. 2003. Delimiting species: a renaissance issue in systematic biology. Trends in Ecology and Evolution 18:462-470.

Sites Jr., J. W., and J. C. Marshall. 2004. Operational criteria for delimiting species. Annual Review of Ecology, Evolution, and Systematics 199-227.

Schoener, T. W. 1968. The Anolis lizards of Bimini: resource partitioning in a complex fauna. Ecology 49:704-726.

Sullivan, J., E. Arellano, and D. S. Rogers. 2000. Comparative phylogeography of Mesoamerican highland rodents: concerted versus independent response to past climatic fluctuations. The American Naturalist 155:755-768.

Thomas, O. 1907. On Neotropical mammals of the genera *Callicebus*, *Reithrodontomys*, *Ctenomys*, *Dasypus*, and *Marmosa*. The Annals and Magazine of Natural History, 7:161-168.

Urbina, S. I., *et al*. 2006. Karyotypes of three species of harvest mice (genus *Reithrodontomys*). The Southwestern Naturalist 51:564-568.

Warren, D. L., R. E. Glor, and M. Turelli. 2008. Environmental niche equivalency versus conservatism: quantitative approaches to niche evolution. Evolution: International Journal of Organic Evolution 62:2868-2883.

Warren, D. L., R. E. Glor, and M. Turelli. 2010. ENMTools: a toolbox for comparative studies of environmental niche models. Ecography 33:607-611.

Yang, Z., and B. Rannala. 2014. Unguided species delimitation using DNA sequence data from multiple loci. Molecular Biology and Evolution 31:3125-3135.

Associated editor: Jake Esselstyn and Giovani Hernández Canchola
Submitted: September 7, 2022; Reviewed: October 26, 2022
Accepted: December 7, 2022; Published on line: January 27, 2023

Appendix 1

Population numbers (corresponding in Figure 2), specimen identification numbers (museum voucher or collector numbers), Collecting locality information; GenBank accession numbers and related clade for each sample of *Reithrodontomys sumichrasti* individuals included in this study. Museum or collector abbreviations are as follows: ASNHC = Angelo State Natural History Collection; BYU = Brigham Young University; CMC = Colección de Mamíferos del CIByC, Universidad Autónoma del Estado de Morelos; MSB = Museum of Southwestern Biology; ROM = Royal Ontario Museum; TTU = Texas Tech University; CWK = C. William Kilpatrick (University of Vermont); JAG = José A. Guerrero (Universidad Autónoma del Estado de Morelos). Country abbreviations are as follows: CR = Costa Rica; GM = Guatemala; HD = Honduras; MX = México; NI = Nicaragua; PN = Panamá. New sequences are denoted by an asterisk.

Pop. Num.	Voucher number	Country: State	Locality	GenBank accession numbers			Clade
				Cyt-b	Fgb-I7	Acp5	
1	BYU15437	MX: Oaxaca	1.5 km S Puerto de la Soledad, 2200 m (18.1623667; -96.9975333)	AF211911			II
	BYU15438			AF211905			II
	BYU16249			HQ269530	HQ269737	HQ269468	II
	BYU15433			HQ269531			II
2	BYU15434	MX: Oaxaca	El Polvorín, 5.3 km turn off Lachao Viejo, 1735 m (16.1999333; -97.1339667)	AF211915			II
	BYU20806			HQ269532	HQ269738	HQ269469	II
	BYU20808			HQ269534			II
	BYU20807			HQ269533	HQ269739	HQ269470	II
3	CMC912	MX: Oaxaca	Finca Copalita, Copalita, 1025 m (15.9655833; 96.4574667)	HQ269535	HQ269740	HQ269471	II
	CMC913			HQ269536			II
	CMC914			HQ269537			II
4	CMC915	MX: Oaxaca	Río Molino, 2353 m (16.0796667; -96.4708833)	HQ269538	HQ269741	HQ269472	II
	CMC991			HQ269539	HQ269742	HQ269473	II
	CMC992			HQ269540	HQ269743	HQ269474	II
	CMC993			HQ269541			II
	CMC994			HQ269542			II
	CMC995			HQ269543			II
	CMC996			HQ269544			II
	CMC997			HQ269545	HQ269744	HQ269475	II
	CMC998			HQ269546			II
	CMC999			HQ269547			II
	CMC1000			HQ269548			II
	CMC1001			HQ269549	HQ269745	HQ269476	II
	CMC1002			HQ269550			II
	CMC1003			HQ269551			II
	CMC1004			HQ269552	HQ269746	HQ269477	II
	CMC1005			HQ269553			II
	CMC1006			HQ269554			II
	CMC1007			HQ269555			II
	CMC1008			HQ269556			II
	CMC1009			HQ269557			II
	CMC1010			HQ269558			II
5	CMC172	MX: Oaxaca	Santa María Yacochi, Cerro Zempoaltepec, 2300 m (17.1583333; -96.0166667)	HQ269559			II
6	CMC1650	MX: Oaxaca	La Cumbre, 1.2 km SE 0.6 km S Agua Fría Juxtlahuaca, 1950 m (17.209; -97.9786667)	HQ269560			II
7	TTU54952	MX: Oaxaca	3.0 mi S. Suchixtepec (16.0166667; -96.4666667)	AF211920			II
8	CMC989	MX: Oaxaca	0.7 km E La Soledad (15.9823; -96.5198167)	HQ269561			II
	CMC990			HQ269562			II
9	CMC734	MX: Oaxaca	La Cumbre, 18.5 km S Sola de Vega, 2175 m (16.4529; -97.00235)	HQ269563			II
10	CWK1009	MX: Oaxaca	Orizaba (17.8333333; -97.2333333)	AF211895			II
11	FAC1112*	MX: Guerrero	6.1 km SW Omiltemi, 2490 m (17.5491667; -99.721)	AF211907			II
	FAC1117*			AF211913			II
	FAC1118			AF211906			II
	FAC1119			AF211908			II
	BYU20801			HQ269564	HQ269747	HQ269478	II
	BYU20802			HQ269565			II
	CWK1019*			AF211921			II
	CWK1025*			AF211901			II
12	BYU20799	MX: Guerrero	3.4 km W Carrizal, 2480 m (17.6004167; -99.8248333)	HQ269566	HQ269748	HQ269479	II
	CMC710			HQ269567			II

13	CMC1628	MX: Guerrero	3 km E El Tejocote, 2620m (17.3048667; -98.6511167)	HQ269568			II
	CMC1629			HQ269569	HQ269749	HQ269480	II
	CMC1630			HQ269570	HQ269750	HQ269481	II
	CMC1631			HQ269571			II
	CMC1632			HQ269572			II
	CMC1633			HQ269573			II
	CMC1634			HQ269574			II
	CMC1635			HQ269575			II
	CMC1636			HQ269576			II
	CMC1637			HQ269579			II
	CMC1638			HQ269580			II
	CMC1639			HQ269581			II
	CMC1640			HQ269582			II
	CMC1641			HQ269583			II
	CMC1642			HQ269584			II
	CMC1643			HQ269585			II
	CMC1644			HQ269586			II
	CMC1645			HQ269587			II
	CMC1646			HQ269577			II
	CMC1647			HQ269578			II
	CMC1648			HQ269588			II
	CMC1649			HQ269589			II
14	TK93354	MX: Guerrero	4 mi SSW Filo de Caballo (17.8166667; -99.6166667)	AY293810			II
	TK93363			AY293811			II
15	BYU20800	MX: Guerrero	1.1 km E Cruz Nueva, 2650 m (17.513483; -100.0295167)	HQ269590	HQ269751	HQ269482	II
	CMC712			HQ269591			II
	CMC713			HQ269592	HQ269752	HQ269483	II
16	BYU15967	MX: Veracruz	La Colonia, 6.5 km W Zacualpan, 6200 ft (20.4666667; -98.3666667)	HQ269594			III
	BYU 15968			AF211916			III
	BYU15969			HQ269595	HQ269754	HQ269485	III
	BYU15970			HQ269596			III
	BYU 15971			AF211902			III
	BYU15972			HQ269593	HQ269753	HQ269484	III
17	CMC873	MX: Veracruz	Las Cañadas, 1340 m (19.1878333; -96.9834)	HQ269597	HQ269755	HQ269486	III
	CMC875			HQ269598	HQ269756	HQ269487	III
	CMC876			HQ269599			III
18	CMC878	MX: Veracruz	3.5 km E Puerto del Aire, 2524 m (18.6715667; -97.3318667)	HQ269600	HQ269757	HQ269488	II
	CMC879			HQ269601	HQ269758	HQ269489	II
	CMC880			HQ269602	HQ269759	HQ269490	II
19	CMC840	MX: Veracruz	2.9 km E Puerto del Aire, 2524 m	HQ269603			III
	CMC843			HQ269604			III
	CMC847			HQ269605			III
	CMC1403			HQ269606			III
	CMC1405			HQ269607			II

20	CWK1007	MX: Veracruz	Xometla, 2615 m (18.97775; -97.1910833)	AF211914			III
	CMC849			HQ269608	HQ269760	HQ269491	III
	CMC850			HQ269609			III
	CMC851			HQ269610			III
	CMC853			HQ269611			III
	CMC854			HQ269612			III
	CMC855			HQ269613			III
	CMC856			HQ269614			III
	CMC857			HQ269615	HQ269761	HQ269492	III
	CMC858			HQ269616			III
	CMC859			HQ269617			III
	CMC860			HQ269618	HQ269762	HQ269493	III
	CMC861			HQ269619			III
	CMC862			HQ269620			III
	CMC863			HQ269621	HQ269763	HQ269494	III
	CMC864			HQ269622			III
	CMC866			HQ269623	HQ269764	HQ269495	III
	CMC867			HQ269624			III
	CMC869			HQ269625	HQ269765	HQ269496	III
	CMC870			HQ269626			III
	CMC871			HQ269627			III
21	CMC1378	MX: Veracruz	Mesa de la Yerba, 3.4 km SW desviación a Mazatepec, 2040 m (19.5593; -97.0185)	HQ269628			III
	CMC1379			HQ269629			III
	CMC1380			HQ269630			III
	CMC1381			HQ269631			III
	CMC1395			HQ269632			III
	CMC1396			HQ269633			III
	CMC1397			HQ269634			III
	CMC1398			HQ269635			III
	CMC1399			HQ269636			III
	CMC1400			HQ269637			III
	CMC1401			HQ269638			III
	CMC1402			HQ269639			III
22	CMC1446	MX: Veracruz	Cruz Blanca, 2180 m (19.4712; -97.0842)	HQ269640			III
	CMC1447			HQ269641			III
	CMC1448			HQ269642			III
	CMC1449			HQ269643			III
23	CMC1476	MX: Veracruz	Xico Viejo, 1756 m (19.4517667; -97.0583)	HQ269644			III
	CMC1477			HQ269645			III
	CMC1478			HQ269646			III
	CMC1480			HQ269648			III
	CMC1481			HQ269649			III
24	CMC1073	MX: Puebla	4.7 km NE Teziutlán, 1750 m (19.8353167; -97.34135)	HQ269650	HQ269766	HQ269497	III
	CMC1074			HQ269651			III
	CMC1075			HQ269652	HQ269767	HQ269498	III
25	CMC1070	MX: Puebla	El Durazno, 0.5 km Libramiento Parada, 1830m (19.8220833; -97.3399833)	HQ269653			III
26	CMC1093	MX: Puebla	3 km W Cerro Chignaulta, 2176 m	HQ269654	HQ269768	HQ269499	III
27	CMC1992	MX: Puebla	Rancho 22 de Marzo, marker 75.8 km Carretera Ahuazotepec-Zacatlán, 2270 m (19.6677; -97.9890333)	HQ269656	HQ269769	HQ269500	III
	CMC1997			HQ269658			III
	CMC2006			HQ269655			III
	CMC2007			HQ269657			III
	CMC2008			HQ269659			III
	CMC2009			HQ269660			III
	CMC2010			HQ269661			III
28	CMC2005	MX: Puebla	Alhuaca, 8 km NE Vicente Guerrero, 2680 m (18.5705167; -97.1660833)	HQ269662			II
29	CMC1711	MX: Puebla	2 km NW Cuautlamingo, 2171 m (19.7678667; -97.5403333)	HQ269663			III

30	CMC1710	MX: Puebla	Los Parajes, 2555 m (19.7664667; -97.4384667)	HQ269664			III
31	CMC1860	MX: Michoacán	11 km NW Coalcomán, 1600 m (18.803; -103.2261667)	HQ269665			IV
	CMC1862			HQ269666			IV
	CMC1863			HQ269667			IV
32	CMC1859	MX: Michoacán	10.9 km NW Coalcomán, 1680 m (18.7966667; -103.2303333)	HQ269668			IV
33	CMC1855	MX: Michoacán	0.8 km NNE Dos Aguas, 2220 m (18.8075; -102.9263333)	HQ269669	HQ269770	HQ269501	IV
34	CMC1856	MX: Michoacán	4.2 km NNE Dos Aguas, 2370 m (18.8358333; -102.9256667)	HQ269670	HQ269771	HQ269502	IV
35	CMC1857	MX: Michoacán	9.2 km NNE Dos Aguas, 2245 m (18.8046667; -102.9775)	HQ269671			IV
36	BYU16242	MX: Michoacán	10 km S Pátzcuaro, 2350 m (19.4535; -101.6027333)	HQ269672			II
	BYU16243			HQ269673			II
	BYU16244			HQ269674			II
	BYU16245			HQ269675			II
	BYU16246			HQ269676			II
	BYU16247			HQ269677	HQ269772	HQ269503	II
37	CMC1870	MX: Michoacán	9.6 km S Pátzcuaro, 2350 m (19.45695; -101.6075833)	HQ269678			II
38	CMC1871	MX: Michoacán	4.9 km S Santa Clara, 2415 m (19.3611667; -101.6116667)	HQ269679			II
	CMC1872			HQ269680			II
39	CWK1014	MX: Michoacán	2.9 mi E Opopeo (19.4; -101.6)	AF211896			II
	CWK1015			AF211923			II
40	CWK1011	MX: Michoacán	9.9 km NW Mil Cumbres, 2820 m (19.6476667; -100.793)	AF211900			II
	CMC1864			HQ269681	HQ269773	HQ269504	II
	CMC1865			HQ269682			II
	CMC1866			HQ269683	HQ269774	HQ269505	II
	CMC1867			HQ269684			II
	CMC1868			HQ269685			II
41	CWK1056	MX: Michoacán	Villa Escalante (19.4; -101.65)	AF211898			II
42	CMC2001	MX: Hidalgo	Río Chíflón, 9.7 km ENE Crucero los Tules, 1750 m (20.4013333; -98.3840833)	HQ269688			III
	CMC2000			HQ269687			III
	CMC2002			HQ269689			III
43	CMC1982	MX: Hidalgo	5 km ENE Crucero los Tules, 2070 m (20.3834; -98.3647333)	HQ269686	HQ269775	HQ269506	III
	CMC2003			HQ269690			III
	CMC2004			HQ269691	HQ269776	HQ269507	III
44	CMC1071	MX: Hidalgo	22 km NE Metepec, 2210 m (20.3158667; -98.23535)	HQ269693			III
	CMC1092			HQ269692	HQ269777	HQ269508	III
45	BYU15417	MX: Hidalgo	La Mojonera, 6 km S Zacualtipan, 2010 m (20.65; -98.6)	HQ269694			III
	BYU15418			HQ269695			III
	BYU15419			HQ269696			III
	BYU15420			HQ269697			III
	BYU 15421			AF211904			III
	BYU 15422			AF211918			III
46	BYU 15415	MX: Hidalgo	El Potrero, 10 km SW Tenango de Doria, 2200 m (20.65; -98.0666667)	AF211899			III
	BYU15416			HQ269699			III
	BYU15414			HQ269698			III
47	CWK1027	MX: Hidalgo	5.0 Km N Zacualtipán (20.65; -98.6)	AF211922			III
48	CWK1036	MX: Hidalgo	0.5 Km N Molango (20.7833333; -98.7166667)	AF211903			III
49	CMC1786	MX: Estado de México	9 km SW Zacualpán, 2400 m (18.6882667; -99.80595)	HQ269703			II
	CMC1787			HQ269700	HQ269778	HQ269509	II
	CMC1788			HQ269701	HQ269779	HQ269510	II
50	BYU17083	MX: Chiapas	Cerro Mozotal, 2930 m (15.4311; -92.3379)	HQ269704	HQ269780	HQ269511	I
	BYU20784			HQ269707	HQ269781	HQ269512	I
	CMC682			HQ269706			I
	BYU17084			HQ269705			I
51	BYU20795	MX: Chiapas	Rancho la Providencia, 1775 m (15.0913333; -92.0831)	HQ269710	HQ269784	HQ269515	I
	BYU20794			HQ269709	HQ269783	HQ269514	I
	CMC694			HQ269708	HQ269782	HQ269513	I

52	CNMA 35505	MX: Chiapas	San Cristobal (16.75; -92.6333333)	AF211909			I
	CNMA 35508			AF211910			I
	CNMA 35514*			AF211917			I
	NMA 35506*			AF211919			I
53	ASNHC2150	MX: Chiapas	9 km S Rayón (17.2; -93)	AF211894			I
	ASNHC2151			AF211897	HQ269785	HQ269516	I
54	TTU82780	MX: Chiapas	Yalentay (16.7333333; -92.775)	HQ269711			I
	TTU82781			HQ269712			I
55	ECOSCM1220	MX: Chiapas	El Vivero, Parque Nacional Lagos de Montebello, 3.55 km NNW El Vivero, 1452 m (16.25; -92.1333333)	HQ269713	HQ269786	HQ269517	I
56	ROM98287	GM: Huehuetenango	10 km NW Santa Eulalia (15.75; -91.4833333)	HQ269714			I
	ROM98383			HQ269715	HQ269787	HQ269518	I
57	ROM98384	GM: Chimaltenango	15 km NW Santa Apolonia (14.7913833; -90.9708333)	HQ269716	HQ269788	HQ269519	I
58	TTU83709	HD: Copán	Picacho (13.9833333; -88.1833333)	HQ269717			I
59	TTU84602	HD: Intibuca	Santa Rosa (14.77; -88.78)	HQ287797			I
60	JAG417	NI: Esteli	Reserva de Miraflor, 3 km SE Miraflor (13.3683667; -86.4023)	HQ269718			I
61	BYU 15246	CR: San José	El Cascajal de Coronado, 1650 m (9.9166667; -84.0666667)	AF211912			I
62	ROM113151	CR: Cartago	Volcán Irazú, Route 8 Hwy Sign 28 km, La Pastora (9.8666667; -83.9166667)	HQ269720	HQ269790	HQ269521	I
	ROM113178			HQ269724			I
	MSB61880			HQ269719	HQ269789	HQ269520	I
	ROM113180			HQ269726			I
	ROM113153			HQ269722	HQ269792	HQ269523	I
	ROM113181			HQ269727			I
	ROM113179			HQ269725			I
	ROM113152			HQ269721	HQ269791	HQ269522	I
	ROM113154			HQ269723			I
63	MSB130128	PN: Chiriqui	Bugaba, Parque Nacional Volcán Baru-Intermedia (8.85; -82.5666667)	HQ269728	HQ269793	HQ269524	I
64*	unavailable	MX: Guerrero	Las Truchas, 3 km SE Carrizal de Bravo, 2400 m (17.359739; -99.489833)	AB618727			II
	unavailable			AB618732			II
65*	unavailable	MX: Guerrero	Carrizal de Bravo, 2.5 km SE, 2400 m (17.609715; -99.820829)	AB618730			II
	unavailable			AB618729			II
66*	CNMA42283	MX: Oaxaca	Municipio Tlahuitoltepec, vicinity Santa María Yacochi, 2,300 m (17.158419; -96.030241)	AY859471			II